New Applications of Measurement Redundancy in High Performance Relative Navigation Systems for Aviation

Samer Khanafseh, Bartosz Kempny and Boris Pervan,
Illinois Institute of Technology, Chicago, IL

ABSTRACT

This paper describes new methods for using measurement redundancy for navigation in two closely related aviation applications: Sea-Based Joint Precision Approach and Landing System (SB-JPALS) and Autonomous Airborne Refueling (AAR). Because of the mobility and physical sensitivity of the reference station (ship or tanker) in each of these applications, higher levels of accuracy, integrity, continuity and availability are required than for similar precision approach applications at land-based airfields. In this paper, two primary sources of redundancy are considered: multiple antenna/receiver configurations for both SB-JPALS and ARR and an additional inter-vehicle ranging measurement for AAR only. Different methods for using these redundant measurements can be designed to enhance navigation accuracy, integrity and continuity. In this paper, we analyze and quantify the tradeoffs for several unique approaches in the implementation of these redundant measurements in the fault free case. In addition, we provide recommendations for the best-suited method for each application.

INTRODUCTION

In this work, two primary sources of redundancy are considered in two closely related aviation applications: Sea-Based Joint Precision Approach and Landing System (SB-JPALS) and Autonomous Airborne Refueling (AAR). The two sources for redundancy relevant in these applications are: multiple antenna/receiver configurations for both SB-JPALS and AAR and an additional inter-vehicle ranging measurement for AAR only. The use of redundant GPS satellites has already been analyzed in prior research and will be exploited in both systems to aid in the carrier cycle resolution process. Different methods for using these redundant measurements can be designed to enhance navigation accuracy, integrity and continuity. In this paper, we analyze and quantify the tradeoffs for several unique approaches that would benefit from measurement redundancy in fault free scenarios.

SB-JPALS is intended to support automatic shipboard landing and AAR will be responsible for navigating Unmanned Air Vehicles (UAV) to tanker airplanes for refueling. Because of the mobility of the reference station (ship or tanker) in each of these applications, higher levels of accuracy are required than for similar precision approach applications at land-based airfields. In addition, to ensure safety and operational usefulness, the navigation architecture must provide high levels of integrity, continuity and availability. Integrity risk is the likelihood of an undetected navigation error or failure that results in hazardously misleading information. Continuity risk is the probability of a detected but unscheduled navigation function interruption after an operation has been initiated. Availability is the fraction of time the navigation function is considered usable (as determined by its agreement with the accuracy, integrity, and continuity requirements) before an operation is initiated. Because of the highly stringent requirements, both systems are based on Carrier Phase Differential GPS positioning (CPDGPS). However in order to benefit from the high precision of CPDGPS the correct resolution of cycles must be ensured.

A number of methods have been used to obtain the cycle resolution. Satellite motion can provide the observability of the cycle ambiguities [1]. Unfortunately the rate of satellite motion is relatively slow in comparison with the time scales of the two analyzed aviation applications. However, carrier measurements at the two frequencies (L1 and L2) can be combined to create a beat frequency measurement with a wavelength of 86cm, generally known as the widelane observable. Because of the longer wavelength, the widelane cycle ambiguities are easier to identify using code phase measurements. Geometry free/divergence free code-carrier filtering is performed continuously for visible

satellites on both the aircraft and the ship/tanker until the aircraft is close to the ship/tanker [2]. Geometry free filtering, by definition, does not depend on the geometry of the satellites or the user location and eliminates most of the nuisance terms and errors. A geometry free measurement of the widelane cycle ambiguity can be formed by subtracting the narrowlane pseudorange from the widelane carrier (which leads to eliminating the geometry-dependable and the nuisance terms [3]). A drawback of the widelane observable is the presence of higher noise with respect to the L1 and L2 carrier phase observables. This can be overcome by filtering the widelane observable over time preceding the final approach.

The outputs of the filtering process are the floating widelane cycle ambiguity estimates. When the aircraft is close to the ship/tanker, the widelane cycle ambiguity estimates (from ship/tanker and aircraft) are combined to form the double difference cycle ambiguity estimates. When the aircraft is close to the tanker/ship, L1/L2 cycle ambiguity estimates ($\Delta\nabla\hat{\mathbf{N}}_{L1}^{ij}$ and $\Delta\nabla\hat{\mathbf{N}}_{L2}^{ij}$) can be extracted with the aid of the geometric redundancy [3]. Finally the cycle ambiguities are fixed using the LAMBDA bootstrap method [4]. The bootstrap rounding process is performed for those ambiguities that can be fixed with a probability of incorrect fix (PIF) that is lower than the predefined requirement. The remaining ambiguities remain floating. With the ambiguities resolved, or partially resolved in this manner, the aircraft calculates its position with centimeter level accuracy.

A potential benefit of using redundant antennas/receivers (for both SB-JPALS and AAR) is the reduction of the highly stringent performance requirements for individual receivers while maintaining the high overall integrity requirement. As we will show, the use of multiple receivers may allow relaxation of the Probability of Incorrect cycle ambiguity Fix (PIF) for individual reference-user receiver pairs. The ability to increase the PIF increases tolerance to higher variances of the raw measurements from the receivers. An additional advantage is a decrease in the required time of measurement filtering prior to cycle resolution. This will allow for shorter mission durations. In this paper the relationships between allowable PIF, receiver performance, and overall system availability are explicitly quantified. However, such use of measurements from redundant antennas assumes that essentially the same set of satellites is visible by both antennas. This might not be the optimal solution for AAR because of the sky blockage that is introduced by the tanker.

In the next sections, we first explain the theory behind the two approaches and then quantify their performance for both SB-JPALS and AAR. Based on the availability results, separate resolutions are made for each application.

FAULT FREE COUPLED ESTIMATION

One of the benefits of having multiple antennas is the access to more measurements. Increasing the number of measurements enables greater accuracy and availability. The relative position vector between the multiple antennas on each vehicle is known because the antennas are fixed on the body of the aircraft/ship, and the attitude information is known through the inertial measurement system. This allows us to bring down measurements to a common reference point on the two vehicles respectively. In practice this doubles (assuming clear sky conditions) the number of code/carrier observables.

The measurement redundancy will be beneficial in resolving cycles in the geometric redundancy step. The double difference carrier observable ($\Delta\nabla\phi_{bc}^{ij}$) between two receivers *b* and *c* and satellites *i* and *j* is given by Equation 1. The line of sight vector is assumed to be the same for the antennas on the the two vehicles due to the short distance between them.

$$\Delta\nabla\phi_{bc}^{ij} = \left(-e^{i} + e^{j}\right)^{T} x_{bc} + \Delta\nabla N_{bc}^{ij} + v_{bc} \qquad (1)$$

where,

$\Delta\nabla\phi_{bc}^{ij}$: the double difference carrier phase observable

e^{i}, e^{j}: the unit line of sight vectors to satellites *i* and *j* respectively

x_{bc}: the vector displacement between receivers *b* and *c*

$\Delta\nabla N_{bc}^{ij}$: the double difference cycle ambiguity

v_{bc}: double difference noise

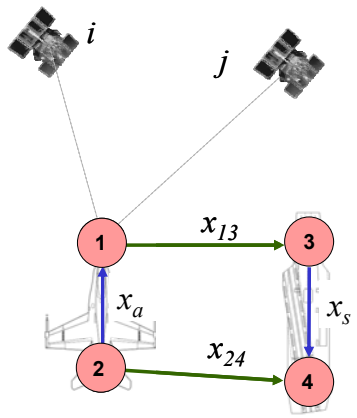

Figure 1: Dual string antenna/receiver configuration

In case of having multiple receivers/antennas we can form multiple pairs of double difference carrier observables. In this work we limit ourselves to two receivers/antennas on the aircraft (marked as 1 and 2 in Figure 1) and two receivers/antennas on the ship/tanker

(marked as 3 and 4 in Figure 1). Therefore, the carrier phase observable for the two processing strings (string 1-3 and string 2-4) can be written as,

$$\Delta\nabla\phi_{13}^{ij} = \left(-e^i + e^j\right)^T x_{13} + \Delta\nabla N_{13}^{ij} + v_{13} \qquad (2)$$

$$\Delta\nabla\phi_{24}^{ij} = \left(-e^i + e^j\right)^T x_{24} + \Delta\nabla N_{24}^{ij} + v_{24} \qquad (3)$$

We note here that in order to benefit from the increased number of measurements we have to establish a common reference point for both the air and ship. As depicted in Figure 1

$$x_{24} = x_{13} + x_a + x_s \qquad (4)$$

where

x_a : the relative vector between receivers 1 and 2 on the aircraft

x_s : the relative vector between receivers 3 and 4 on the ship/tanker

Because the two vectors (x_a and x_s) are known, thanks to the attitude information provided by the inertial systems, we can rewrite Equation 3 as,

$$\Delta\nabla\phi_{24}^{ij} = \left(-e^i + e^j\right)^T \left(x_{13} + x_a + x_s\right) + \Delta\nabla N_{24}^{ij} + v_{24} \qquad (5)$$

As a result, the measurements from both strings are coupled through the relative position vector x_{13}. In addition, we have successfully increased the number of measurements that allows us to estimate the relative vector between the aircraft and ship/tanker with a greater precision. The final equation can be expressed in a matrix form as,

$$\begin{bmatrix} \Delta\nabla\boldsymbol{\varphi}_{13} \\ \Delta\nabla\boldsymbol{\varphi}_{24} - \mathbf{G}\mathbf{x}_a - \mathbf{G}\mathbf{x}_s \end{bmatrix} = \begin{bmatrix} \mathbf{G} & \mathbf{I} & \mathbf{0} \\ \mathbf{G} & \mathbf{0} & \mathbf{I} \end{bmatrix} \begin{bmatrix} \mathbf{x}_{13} \\ \Delta\nabla\mathbf{N}_{13} \\ \Delta\nabla\mathbf{N}_{24} \end{bmatrix} + \begin{bmatrix} \mathbf{v}_{13} \\ \mathbf{v}_{24} \end{bmatrix} \qquad (6)$$

where

$$\mathbf{G} = \left(-e^i + e^j\right)^T$$

In this method we have assumed that there is no correlation present between the measurements from the receiver pairs on the air and ship respectively, although this would have to be addressed in a future analysis.

In order to estimate the position vector precisely, the cycle ambiguities must be resolved. In this work, this is achieved using the LAMBDA bootstrap method, where the estimated ambiguities covariance matrix is decorrelated and then fixed [4]. As in the case of single air/ship receiver pair we set the probability of incorrect fix to be 10^{-8}. This allows us to maintain the integrity requirement associated with the ambiguity resolution.

FAULT FREE DECOUPLED ESTIMATION WITH INCORRECT CYCLE FIX DETECTION

The second proposed method that utilizes additional measurements from multiple receivers assumes that independent estimation is performed on the receiver pairs. However, the additional measurements are used to relax the PIF requirement. The relaxation of the PIF requirement expedites the cycle resolution and, hence enhances the availability. However, relaxing PIF introduces a new source of faults (incorrect fixes) which are caused by signal noise rather than actual failures. In order to maintain the overall fault-free integrity requirement associated with cycle ambiguity resolution, a fault-free incorrect-fix detection monitor is necessary. The monitor will compare individual measurements directly between the two strings. The derivation of the test statistic starts by differencing Equation 3 from Equation 2 as shown in Equation 7.

$$\Delta\nabla\phi_{13}^{ij} - \Delta\nabla\phi_{24}^{ij} = \left(-e^i + e^j\right)^T \left(x_{13} - x_{24}\right) + \Delta\nabla N_{13}^{ij} - \Delta\nabla N_{24}^{ij} + v_{13} - v_{24} \qquad (7)$$

Recalling the relationship between vectors x_{13} and x_{24} (from Equation 4), Equation 7 can be rewritten in terms of the estimated integers only (and not the estimated position) as,

$$\Delta\nabla\phi_{13}^{ij} - \Delta\nabla\phi_{24}^{ij} = -\left(-e^i + e^j\right)^T \left(x_a + x_s\right) + \Delta\nabla N_{13}^{ij} - \Delta\nabla N_{24}^{ij} + v_{13} - v_{24} \qquad (8)$$

After fixing the ambiguities, the test statistic S^{FF} can be calculated using Equation 9,

$$S^{FF} = \Delta\nabla\phi_{13}^{ij} - \Delta\nabla\phi_{24}^{ij} + \left(-e^i + e^j\right)^T \left(x_a + x_s\right) - \Delta\nabla N_{13}^{ij} + \Delta\nabla N_{24}^{ij} = v_{13} - v_{24} \qquad (9)$$

If the ambiguities were fixed correctly, S^{FF} should amount to zero mean and the random noise term $v_{13} - v_{24}$. Therefore, in order to detect if the cycles have been fixed correctly, we need to pass the S^{FF} through a monitor.

In order to compute how much we can relax the PIF requirements, we need to establish a relationship between the PIF and the Probability of Missed Detection (PMD). The fault-free integrity requirement for SB-JPALS and AAR is assumed to be 10^{-7}. For the purpose of this analysis, we assume that 10% of this budget is allocated to the cycle resolution. Therefore the tolerable probability of an incorrect fix occurring without detecting it is given by:

$$P(IF \cap MD) = 10^{-8} \tag{10}$$

It is worth noting here that in the case of the coupled estimation discussed previously, due to the fact that we had no means of incorrect fix detection, the PIF needs to be set to 10^{-8} to ensure integrity. In the case of dual string decoupled estimation, if an incorrect fix occurred, we have no means of isolating the string where the incorrect fix took place. Therefore the total probability of incorrect fix is given by,

$$P(IF) = P(IF_{13} \cup IF_{24}) \tag{11}$$

Substituting Equation 11 into Equation 10 we get,

$$P(IF \cap MD) = P((IF_{13} \cup IF_{24}) \cap MD) \tag{12}$$

Expanding Equation 12,

$$\begin{aligned} &P(MD \cap IF) = P(MD \cap (IF_{13} \cup IF_{24})) = \\ &P[IF_{13}] \cdot P[\overline{IF}_{24}] \cdot P[MD \mid (IF_{13} \cap \overline{IF_{24}})] \\ &+ P[\overline{IF_{13}}] \cdot P[IF_{24}] \cdot P[MD \mid (\overline{IF_{13}} \cap IF_{24})] \\ &+ P[IF_{13}] \cdot P[IF_{24}] \cdot P[MD \mid (IF_{13} \cap IF_{24})] \end{aligned} \tag{13}$$

We assume here that the probability of incorrect fix in strings 1-3 ($P[IF_{13}]$)and string 2-4 ($P[IF_{24}]$) are equal. The assumption is valid because *P[IF]* is an allocation. In addition, the conservative assumption that $P[\overline{IF}_{13}] = P[\overline{IF}_{24}] \approx 1$ is used because PIF is very small compared to $P[\overline{IF}]$. In the last term of the equation, we assume that if an incorrect fix occurred simultaneously on the two strings the probability of not detecting it is equal to $P[MD \mid (IF_{13} \cap IF_{24})] = 1$. As a result,

$$\begin{aligned} &P(IF \cap MD) = \\ &\quad 2 \cdot P[IF_{13}] \cdot P[MD \mid (IF_{13} \cap \overline{IF}_{24})] \\ &\quad + P[IF_{13}]^2 \end{aligned} \tag{14}$$

By substituting equation 10 in equation 14, the required PMD on each string can be calculated for a given PIF using Equation 15.

$$P[MD \mid (IF_{13} \cap \overline{IF}_{24})] = \frac{10^{-8} - P[IF_{13}]^2}{2 \cdot P[IF_{13}]} \tag{15}$$

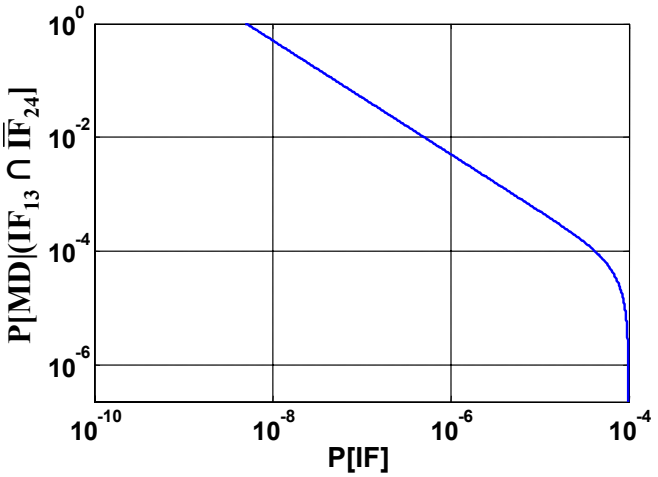

Figure 2: Required PMD versus allowable PIF

The relationship expressed in Equation 15 between the required PMD and allowable PIF is shown in Figure 2. From Figure 2, we can deduce that if we want to relax the PIF requirement to 10^{-4} we need to ensure a PMD that is roughly lower than 10^{-6}. We note that the curve asymptotically converges to 10^{-4} but will in fact never reach it. In order to find whether we can ensure such a probability of missed detection (PMD), the relationship between the PMD and a Minimum Detectable Error (MDE) of 19cm for L1 is established. The MDE value corresponds to a full L1 cycle because fixing a cycle ambiguity incorrectly will result in biases that are in cycle increments (with one cycle being the minimum fault caused by an incorrect fix). The relevant threshold (*T*) in this case is dependent on the double difference carrier phase standard deviation ($\sigma_{\Delta\nabla\phi}$) and an availability requirement of 99% which corresponds to an availability multiplier (*K*) of 2.58 (Equation 16).

$$T = \sqrt{2}\ K\ \sigma_{\Delta\nabla\phi} \tag{16}$$

The probability of missed detection (PMD) that is achievable with the MDE and the availability requirement is found to be 5×10^{-23} which is much lower than 10^{-6} that is necessary for PIF relaxation to 10^{-4} (See Figure 2). We can therefore use 10^{-4} for each string and then apply the prescribed monitor to detect any incorrect fix. As a result, this approach maintains the incorrect fix integrity risk requirement of 10^{-8}.

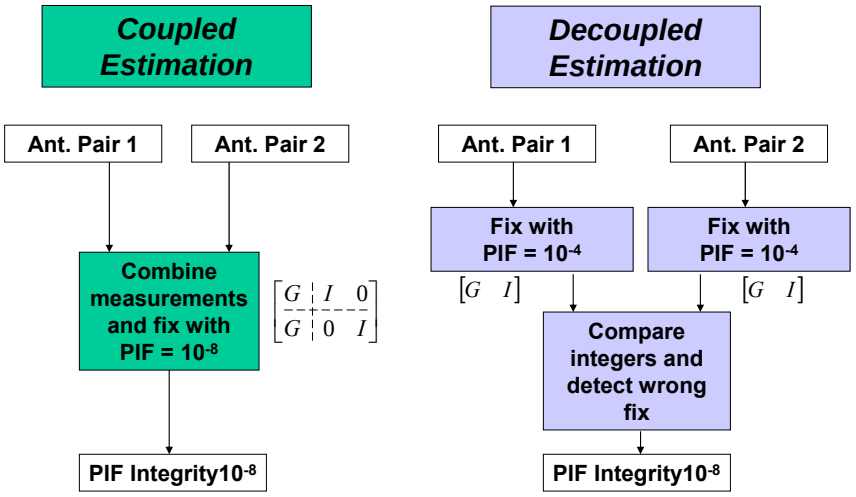

Figure 3: Coupled estimation and decoupled estimation flow charts

The flow chart shown in Figure 3 summarizes the two approaches utilizing redundant measurements. Both approaches assume fault free conditions. In the following sections we present simulated results that apply the two approaches to both SB-JPALS and AAR. In addition, a comparison between the single string individual estimation, coupled estimation and decoupled estimation is conducted based on availability results.

JPALS AVAILABILITY ANALYSIS RESULTS

The benefits of redundant measurements were quantified for SB-JPALS mission using a covariance analysis simulation for terminal navigation of aircraft. All three approaches were compared: the single string individual estimation with a PIF of 10^{-8}, the fault free coupled estimation with a PIF of 10^{-8} and the fault free decoupled estimation with incorrect fix detection and a relaxed PIF of 10^{-4}.

In this work, *availability* is defined as the percentage of time under which the Vertical Protection Level (VPL) is smaller than a Vertical Alert Limit (VAL) of 1.1 m. VAL is an integrity requirement representing the tolerable error. The VPL is a function of the integrity risk (10^{-7}), the satellite geometry, and precision of GPS measurements. The VPL is generated via a covariance analysis of the proposed architecture. The processing starts by prefiltering the widelane observables in both the tanker and receiver aircraft. In this analysis, a maximum prefiltering period of 15 minutes is assumed to generate floating estimates of the widelane cycle ambiguities. The floating widelane ambiguities from the tanker are combined with the aircraft floating ambiguities to form the double difference widelanes. Geometric redundancy is applied and the LAMBDA bootstrap method is used to fix those widelane and L1 and L2 integers which meet the required PIF. After the integer fixing, the position of the receiver aircraft can be estimated. The vertical component of the position estimation standard deviation (σ_V) is calculated and used to generate VPL. VPL is calculated by multiplying σ_V by the integrity risk multiplier corresponding to the integrity risk requirement (5.33 in the case of 10^{-7} integrity risk).

Using single difference carrier phase standard deviation of 1cm and different values of code single difference standard deviations (σ_{PR}), the availability is calculated and shown in Figures 4 and 5. These results (and those that follow) assume a first order Gauss-Markov measurement error model with a time constant of 5 seconds and 60 seconds for air and ship respectively. A standard 24 satellite constellation without outages is used. The simulated locations are chosen to be the Central Atlantic Ocean (latitude: 25°N, longitude: 30°W) and the Pacific Ocean (5°n, 135°W). The SB-JPALS mission will incorporate Controlled Reception Pattern Antennas (CPRA) that may introduce a bias in the widelane observable [5]. Therefore, for demonstration purposes, a bias of 6cm (1σ) was introduced to the widelane observables.

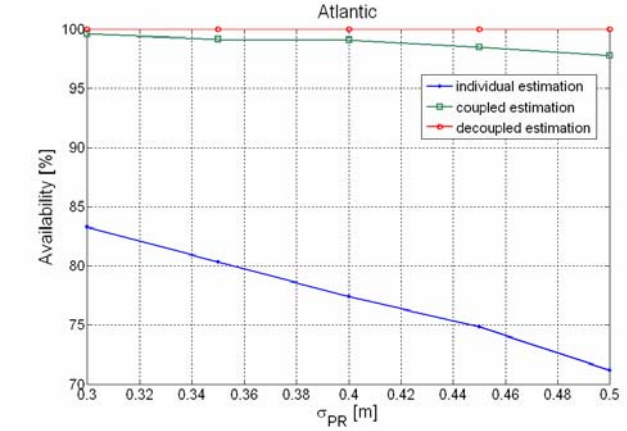

Figure 4: Availability results for the central Atlantic Ocean location

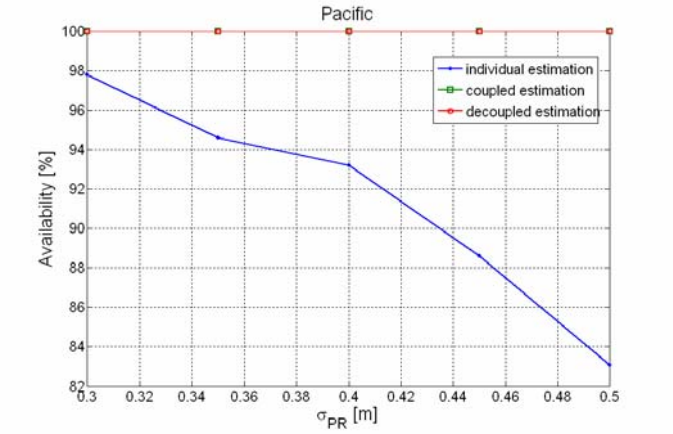

Figure 5: Availability results for the Pacific Ocean location

For both locations the single string individual estimation does not meet 99% availability. This differs from previous results [3] because of changes in simulation parameters, namely introducing antennas biases and a shortened prefiltering time of 15 minutes. The coupled dual string estimation considerably increased availability, while the decoupled estimation with IF detection showed the best results of a 100% availability for the two locations and the simulated range of the code variance with shorter prefiltering time. Clearly the results are sensitive to the chosen locations, but in both cases the implementation of the two approaches greatly enhanced the achievable availability. The recommended approach for the SB-JPALS mission is the decoupled dual string estimation with incorrect fix detection. The fact that the mission nominally takes place under clear sky conditions allows us to form double differences for all the satellites currently in view, which will not be the case for AAR due to sky blockage. Therefore, AAR availability analyses using the prescribed methods are quantified in the following section.

AAR AVAILABILITY RESULTS

As mentioned earlier, the AAR mission is different from SB-JPALS mission because of the severe sky blockage that is introduced by the tanker. In previous work [6], a detailed blockage model was developed utilizing the 3D shape of a KC-135 tanker (Figure 6). In addition, the AAR navigation problem was analyzed in detail and the navigation performance was quantified by conducting a worldwide global availability analysis. The results showed that availability and continuity are highly affected by the tanker blockage for a UAV with a single antenna. However, when the UAV is equipped with multiple antennas (as planned), the situation is expected to improve considerably. When the UAV is at the refueling point location, different antennas may have access to different sets of satellites. Each set might not individually have enough satellites for a position estimate. However, using the attitude information provided by the inertial system onboard the UAV, both sets of measurements can be blended together in one set that has enough information to estimate an accurate position. Therefore, satellites from different antennas can be combined and used to enhance the continuity, accuracy, and availability of the system. In this regard, the resulting performance improvement gained using the extra antennas will be quantified analytically.

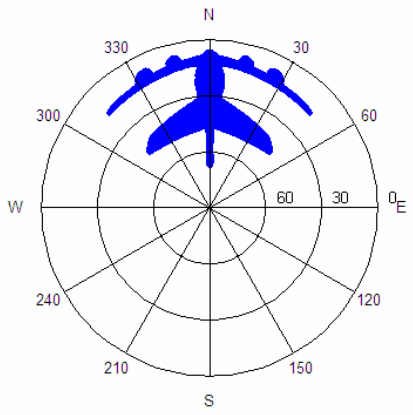

Figure 6: Kc-135 blockage shadow as seen from an antenna 98" aft the refueling point.

The same analysis that was carried out for SB-JPALS in the previous section is conducted to quantify the impact of multiple antennas on AAR. Both the coupled estimation and decoupled estimation methods are compared to the individual estimation method. In this analysis a straight and level refueling pattern is assumed. In addition, a 27 satellite constellation (24+3 spare) [7] with a 3^{o} elevation mask and a carrier phase single difference sigma of 1.0 cm are assumed. Availability is quantified with respect to σ_{PR}, which is varied from 30cm to 1.0m in 5cm increments. In the individual estimation case, a single antenna is located 98" aft the refueling port and the Probability of Incorrect Fix (PIF) is set to 10^{-8}.

As discussed earlier, in the case of the decoupled estimation, only common satellites from both antennas can be processed. Since the blockage by the tanker is sensitive to antenna location, the two antennas are placed far apart. In this case, one antenna is placed at the refueling port and the other antenna is 98" aft. Processing common satellites can be represented as a union between the blockage shadows from both antennas as seen in Figure 7. Using geometric redundancy, common satellites are processed and L1/L2 ambiguities are estimated. The estimated L1/L2 ambiguities are fixed using LAMBDA bootstrap method with a 10^{-4} PIF constraint. In coupled estimation, all visible satellites by both antennas (common and uncommon) are processed

and used at the geometric redundancy step to estimate L1/L2 cycle ambiguities. These ambiguities are fixed with 10^{-8} PIF.

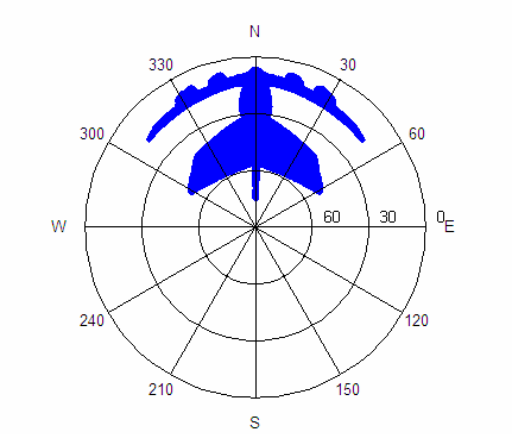

Figure 7: Blockage shadow representation of the decoupled estimation case.

The availability results for decoupled and coupled estimation are compared to the individual estimation (single string) in Figure 8. The first observation is that the availability, for σ_{PR} less than 40 cm, of the individual estimation is higher than that of the dual string decoupled estimation. Although this contradicts the availability results introduced earlier for SB-JPALS case, it can be explained by the blockage of the tanker. Decoupled estimation can only process common satellites from both antennas. This might not be the optimal way of processing for AAR because in the presence of the tanker blockage, different antennas have access to different satellites. In particular, the number of common visible satellites will generally be less than the satellites visible by an individual antenna, which in turn degrades the availability. However, the dual string decoupled estimation is less sensitive to larger σ_{PR} compared to single string individual estimation. This is because in the decoupled estimation, a lower PIF (10^{-4}) than that of the single string individual estimation (10^{-8}) is used, which expedites cycle resolution. On the other hand, the coupled estimation availability is higher than both the individual estimation and the decoupled one. The coupled estimation processes all satellites in view which might be more than what individual estimation processes. This result is different than JPALS because the tanker blockage is driving availability in AAR.

In summary, although the decoupled estimation has lower availability than the individual case for low sigma code, it is more robust to receiver noise (larger σ_{PR}). In addition, although the dual string decoupled estimation produces the best availability for JPALS, the dual string coupled estimation provides the best performance for AAR. This is explained by the fact that the difference between JPALS and AAR is the tanker blockage, which is driving availability in the latter case. So far, the availability analysis was conducted for a straight and level refueling mission. However, in reality, in many refueling missions banks and turns can not be avoided. Therefore, a more accurate model for the AAR mission is described below.

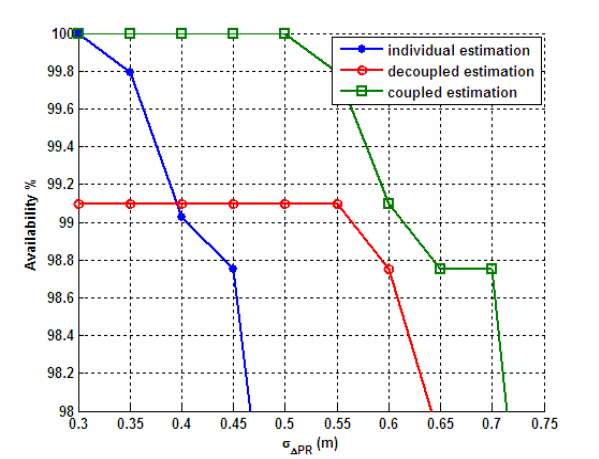

Figure 8: Availability results for AAR

RACE TRACK REFUELING MISSION

The tanker aircraft usually flies in a race track pattern that is limited by the refueling airspace. The race track pattern consists of two straight legs and two turn legs as shown in Figure 9. If the straight leg (marked as 1 or 3) is long enough to refuel the UAV aircraft, a straight and level refueling mission is conducted. If the airspace is small or the refueling time exceeds the straight leg time, a race track refueling becomes necessary. In this work, 14 minutes race track missions are used in the simulation, with five minutes of straight legs and two minutes of turn legs. During the race track refueling, specifically in the turn legs (marked as 2 and 4) and while the UAV stays in contact position below the tanker, it banks and performs a turn maneuver. During the bank, the horizon line of the UAV (zero elevation line with respect to the UAV) will block a certain sector in the sky (Figure 10). i.e., satellites that have negative elevation angle with respect to the UAV antenna are considered blocked. The turn maneuver will sweep both the tanker and the horizon blockages 180° through the sky. This is expected to cause extreme satellite outages and as a result a tremendous degradation to the GPS accuracy.

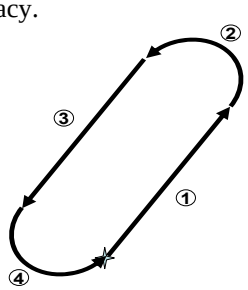

Figure 9: Race track refueling

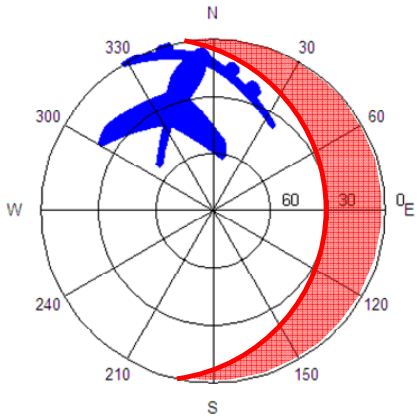

Figure 10: Sky blockage illustration for the UAV during a 30° bank.

The same navigation algorithm that has been used in the straight and level refueling is used here. However, because the blockage and the satellite geometry do not change significantly in straight and level refueling, VPL_{H0} was calculated once (after the fixing the cycle ambiguities). In the case of the race track simulations, the blockage movement at different stages through the race track will affect the visible-satellites geometry. As a result, VPL_{H0} will be changing at each epoch. To account for the geometry change, the availability analysis is performed by simulating 1440 race tracks (one race track per minute during 24 hours). The simulation is executed at a 1Hz rate through the race track. In addition, a 30° elevation mask is applied during the 20-minute prefiltering period. Although this might be considered a conservative assumption, it is necessary in order to account for the maneuvers that the UAV performs during the approach. After prefiltering for 20 minutes, the elevation mask is dropped to 3 degrees and the straight and level blockage model is applied. At this point, the geometric redundancy is executed and L1/L2 cycle ambiguities are estimated for the visible satellites. After fixing the ambiguities using LAMBDA bootstrap with a specific PIF (which differs for the coupled and decoupled estimation methods), relative positioning is applied and VPL_{H0} is calculated.

In race track refueling, the movement of the tanker blockage in the sky will cause different satellites to be blocked at different times. Therefore, if a fixed satellite is blocked there is no means to fix it again. As a result, the positioning accuracy is degraded with time without any means of regaining the lost satellites. In order to be able to fix the new satellites and regain the blocked ones, a parallel track processing is proposed. Two parallel tracks are running at each epoch: the first track calculates the position using the pre-fixed integers, and the second one re-executes the geometric redundancy and fixes the estimated cycle ambiguities. It should be mentioned that the re-execution of the geometric redundancy does not take benefit of the previously estimated or fixed ambiguities. This is necessary to maintain the integrity of the fixing algorithm and the architecture. VPL_{H0} using the current fixed satellites is compared to the VPL_{H0} using the pre-fixed ones. If the current VPL_{H0} is lower than the pre-fixed one, the algorithm replaces the pre-fixed integers with the current fixed ones and uses them to estimate VPL_{H0}. This approach is capable of regaining the blocked satellites, assures the best performance, and is more robust to changes in satellite geometry caused by the blockage. Although this approach can be used in the straight and level refueling architecture, it is not necessary because the visible satellite geometry does not change significantly throughout the mission.

In this analysis, each race track is marked available or unavailable based on VPL_{H0} and VAL. Specifically, the race track is considered unavailable if VPL_{H0} is greater than VAL for a period of time that is longer than the *coasting time*. Coasting time is defined as the time the Inertial Navigation System (INS) can bridge system outages. In previous work [6], it was assumed that the integrated INS system would be capable of bridging outages of up to one minute in duration. Here, the availability is quantified as a function of the coasting time (Figure 11) while fixing sigma code to 30 cm. Since each race track is simulated at 1Hz and the availability is calculated based on 1440 race tracks, the race track availability simulation is computationally time consuming. Therefore, only a race track oriented at an azimuth of 30° is processed in this work. Figure 11 shows the great improvement that the coupled estimation has versus the decoupled and the individual estimations. It is also clear that the availability is very sensitive to the coasting time. In addition, even when coasting is 60 seconds, both the decoupled and coupled estimation availability do not reach 99%. Therefore, a three antenna configuration is proposed to enhance the availability to 99% requirement.

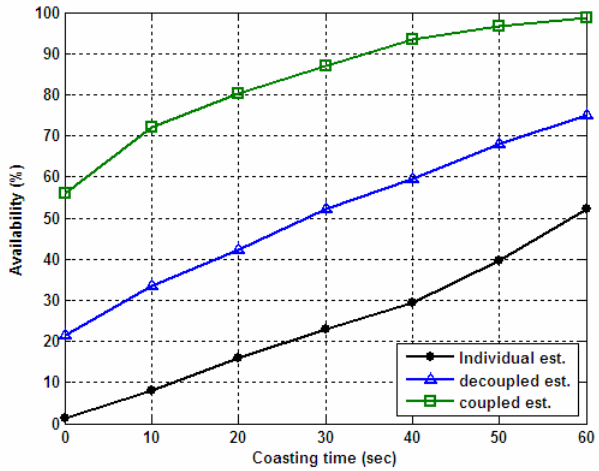

Figure 11: Race track availability results

Placement of the three antennas on the UAV must be optimized to reduce the tanker blockage effect. For example, from a blockage point of view, aligning the three antennas on the UAV body axis will not be significantly different than two antennas at the extreme points of the UAV. However, if two of the antennas are placed on the wings at a sufficient distance, the fuselage part of the tanker blockage can be eliminated (Figure 12). Eliminating the fuselage will improve race track availability by reducing the number of blocked satellites during the turns. However, the antennas must be placed on a rigid area on the wings to avoid flexure. In this work, the Boeing X-45C is used as a basis for determining the antenna locations. The blockage shown in Figure 12 is created by fixing the front antenna at the refueling port and placing the back antennas 98" aft of the front one and 200" apart. The race track availability analysis (discussed above) is then performed on the three antenna case. Figure 13 shows the increase in availability gained by using three antennas. In fact, the requirement on coasting time can be relaxed from 60 to 40 seconds while maintaining availability higher than 99% using coupled estimation with three antennas.

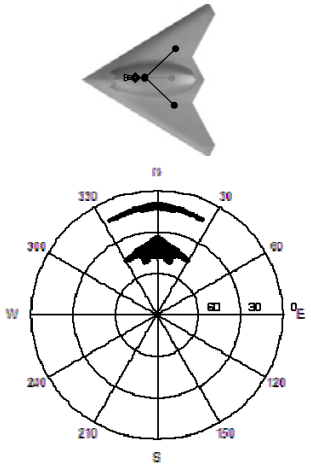

Figure 12: Three antenna configuration and the corresponding blockage

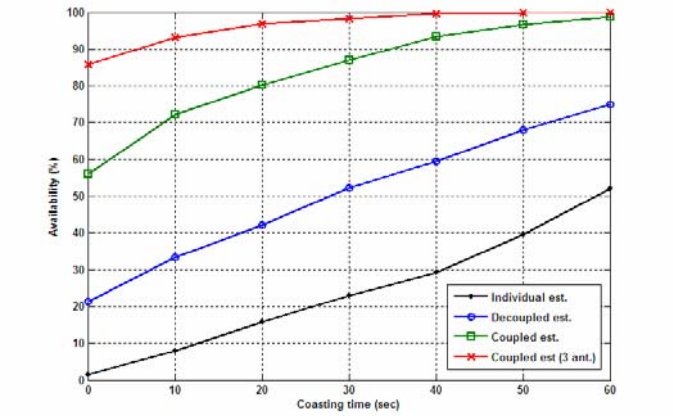

Figure 13: Availability result with 3 antennas

INTER-VEHICLE RANGING MEASUREMENT REDUNDANCY

Additional ranging instruments may provide another source of measurement redundancy for AAR. Specifically, the AAR system will use Tactical Targeting Network Technology (TTNT) as a data link medium. It has been proposed that using TTNT, the potential exists to extract ranging measurements between the tanker and the UAV. The additional ranging measurement would provide an additional line of sight measurement in the direction of the blocked satellites (in the tanker shadow). Therefore, the system will be more robust to satellite blockages caused by the tanker, and the availability and continuity of precision navigation should be improved. The improvement in availability resulting from the use of TTNT is quantified below.

To evaluate the effect of ranging augmentation, we assume the existence of a TTNT ranging signal originating at the belly of the KC-135 tanker (at the refueling boom root) and having a measurement ranging standard deviation of 15 cm. In this analysis, the UAV's TTNT antenna is assumed to be at the refueling port. Although the assumed error standard deviation for the TTNT measurement is relatively high compared to the GPS carrier phase noise, as we will show, the addition of the measurement originating from the center of the blockage has significant impact on position quality.

The TTNT ranging measurement (r) is related to the relative position vector ($\mathbf{x}$) by the lever arm ($\mathbf{L}_T$) between the GPS antenna and TTNT transceiver (Equation 17),

$$r = \left\| \mathbf{x}_{13} + \mathbf{L}_T \right\| + \varepsilon_r \qquad (17)$$

where,

r: TTNT range measurement
$\mathbf{x}_{13}$: tanker-UAV relative position vector
$\mathbf{L}_T$: TTNT-GPS antenna lever arm on the tanker
ε_r: TTNT range measurement noise

Equation 17 can be linearized using the previous estimate of $\mathbf{x}_{13}$ ($\mathbf{x}_0$) to result in,

$$\left(r - \mathbf{1}^T \mathbf{L}_T\right) = \mathbf{1}^T \mathbf{x}_{13} + \varepsilon_r \qquad (18)$$

where,

$\mathbf{1}^T$: the TTNT tanker-UAV transceivers line of sight vector (based on $\mathbf{x}_0$)

Equation 18 can be used to couple the TTNT measurement with the GPS measurement in Equation 2 and 6. The final integrated system can be represented in matrix form as in Equation 19 and 20 for the single string and dual string (coupled) systems respectively.

$$\begin{bmatrix} \nabla\Delta\boldsymbol{\varphi}_{13}^{ij} \\ r - \mathbf{1}^T \mathbf{L}_T \end{bmatrix} = \begin{bmatrix} \mathbf{G} & \mathbf{I} \\ \mathbf{1}^T & \mathbf{0} \end{bmatrix} \begin{bmatrix} \mathbf{x}_{13} \\ \nabla\Delta\mathbf{N}_{13}^{ij} \end{bmatrix} + \begin{bmatrix} \boldsymbol{\varepsilon}_{13}^{ij} \\ \varepsilon_r \end{bmatrix} \quad (19)$$

$$\begin{bmatrix} \nabla\Delta\boldsymbol{\varphi}_{13}^{ij} \\ \nabla\Delta\boldsymbol{\varphi}_{24}^{ij} - \mathbf{G}\left(\mathbf{x}_a + \mathbf{x}_s\right) \\ r - \mathbf{1}^T \mathbf{L}_T \end{bmatrix} = \begin{bmatrix} \mathbf{G} & \mathbf{I} & \mathbf{0} \\ \mathbf{G} & \mathbf{0} & \mathbf{I} \\ \mathbf{1}^T & \mathbf{0} & \mathbf{0} \end{bmatrix} \begin{bmatrix} \mathbf{x}_{13} \\ \nabla\Delta\mathbf{N}_{13}^{ij} \\ \nabla\Delta\mathbf{N}_{24}^{ij} \end{bmatrix} + \begin{bmatrix} \boldsymbol{\varepsilon}_{13}^{ij} \\ \boldsymbol{\varepsilon}_{24}^{ij} \\ \varepsilon_r \end{bmatrix} \quad (20)$$

Using TTNT, the navigation architecture will be able to estimate the relative position with three satellites at least instead of four (without TTNT). This in turn would improve the availability for both single string individual estimation and dual string coupled estimation as seen in Figure 14. For the single string individual estimation case, availability improved from 52% for a coasting time of 60 seconds to 88% using TTNT. For dual string coupled estimation case, the availability improved from 98.7% at a coasting time of 60 seconds to 99.9% (figure 15). With the assumed requirements for AAR, a single string individual estimation with race track refueling is not enough to provide availability of more than 90% even if an additional ranging measurement (TTNT) is used. On the other hand, if dual string coupled estimation with TTNT is used, only 50 seconds of coasting time is needed to provide availability that exceeds 99%.

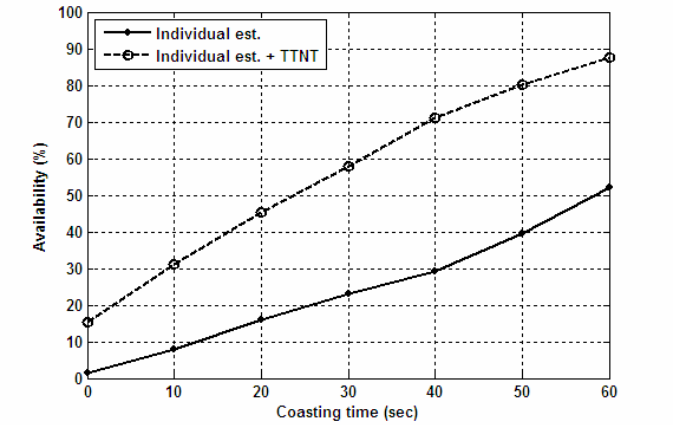

Figure 14: Availability results for single string and single string with TTNT ranging measurement

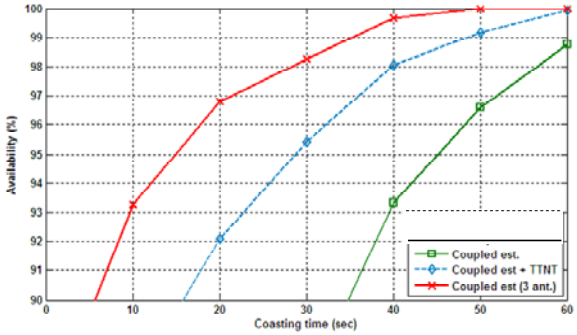

Figure 15: Availability results for coupled, coupled with TTNT and three coupled antennas

CONCLUSIONS

This work describes several new approaches for using redundant measurements to improve the navigation performance of SB-JPALS and AAR. The main methods explored are: blending of measurements from different antennas to form a single set that enhances availability, using common satellites from different antennas to relax PIF requirements, which enhances availability while maintaining the integrity requirement, and using TTNT as an additional measurement to enhance accuracy and availability. For SB-JPALS (a clear sky application), the optimal way of processing the redundant measurements is decoupled estimation with lower PIF while implementing an incorrect fix monitor. In AAR, the blockage is the main driver for availability. Therefore, antenna/receiver redundancy is necessary if race track refueling missions are executed. Specifically, to meet the availability requirement, coupled estimation for two antennas with TTNT ranging augmentation is recommended. If TTNT ranging measurements are not available, coupled estimation with three antennas is recommended.

REFERENCES

[1] P. Misra, and P. Enge, *Global Positioning System Signals, Measurements, and Performance*, Ganga-Jamuna Press, Lincoln, MA, 2001

[2] S. Dogra, J. Wright and J. Hansen, "Sea-Based JPALS Relative Navigation Algorithm Development," *Proceedings of the Institute of Navigation 2005 GNSS Meeting,* Long Beach, CA, Sept. 13-16, 2005

[3] M. Heo, B. Pervan, S. Pullen, J. Gautier, P. Enge, and D. Gebre-Egziabher, "Robust Airborne Navigation Algorithm for SRGPS," *Proceeding of the IEEE Position, Location, and Navigation Symposium (PLANS '2004*), Monterey, CA, April 2004.

[4] P. Teunissen, D. Odijk, and P. Joosten, "A Probabilistic Evaluation of Correct GPS Ambiguity Resolution," *Proceedings of the 11th International Technical Meeting of the Satellite Division of the Institute of Navigation (ION GPS 1998)*, Nashville, TN, September 15-18, 1998

[5] U. S. Kim, "Analysis of Carrier Phase and Group Delay Biases Introduced by CRPA Hardware," *Proceedings of the Institute of Navigation 2005 GNSS Meeting,* Long Beach, CA, Sept. 13-16, 2005

[6] S. Khanafseh, B. Pervan, J. Gautier, P. Enge and G. Colby, "Validation of Autonomous Airborne Refueling Algorithms Using Flight Test Data," *Proceedings of the Institute of Navigation 2005 GNSS Meeting,* Long Beach, CA, Sept. 13-16, 2005

[7] P. Massatt, F. Fritzen and M. Perz, "Assessment of the Proposed GPS 27-Satellite Constellation," *Proceedings of the 16th International Technical Meeting of the Satellite Division of the Institute of Navigation (ION GPS/GNSS 2003),* Portland, OR, September 2003